Brazilian Journal
of Chemical
Engineering

ISSN 0104-6632
Printed in Brazil
www.abeq.org.br/bjche

Vol. 22, No. 03, pp. 433 - 442, July - September, 2005

A Cu/Al-MCM-41 MESOPOROUS MOLECULAR SIEVE - APPLICATION IN THE ABATEMENT OF NO IN EXHAUST GASES

M. S. Batista[1], R. A. A. Melo[2], M. Wallau[1] and E. A. Urquieta-González[1*]

[1]Departamento de Engenharia Química, Universidade Federal de São Carlos,
Phone (16) 260-8202, Fax (16) 260-8286,
Cx. P. 676, CEP 13565-905, São Carlos - SP - Brazil
E-mail: urquieta@power.ufscar.br
[2]Laboratório de Catálise e Desenvolvimento de Materiais, Centro Universitário do Sul de Minas,
Av. Cel. José Alves 256, CEP 37010-540, Varginha - MG, Brazil

(Received: January 12, 2003 ; Accepted: January 11, 2005)

Abstract - Propane oxidation and reduction of NO to N_2 with propane under oxidative conditions on a Cu-Al-MCM-41 mesoporous molecular sieve and Cu-ZSM-5 zeolites were studied. Both types of catalysts were prepared by ion exchange in aqueous solutions of copper acetate and characterised by X-ray diffraction (XRD), nitrogen sorption measurement, diffuse reflectance ultra-violet spectroscopy (DRS-UV), diffuse reflectance infra-red Fourier transform spectroscopy (DRIFTS) of the adsorption of CO on Cu^+ and temperature-programmed reduction with hydrogen (H_2-TPR). The NO reduction was performed between 200 and 500 ^oC using a GHSV = 42,000 h^{-1}. H_2-TPR data showed that in the prepared Cu-Al-MCM-41 all the Cu atoms are on the surface of the mesopores as highly dispersed CuO, which results in a decrease in specific surface area and in mesopore volume. H_2-TPR together with DRIFTS data provided evidence that in Cu/ZSM-5 catalysts, Cu atoms are found as two different Cu^{2+} cations: Cu_α^{2+} and Cu_β^{2+}, which are located on charge compensation sites, and their thermo-redox properties were different from those of Cu atoms in Cu-Al-MCM-41. The specific activity of the Cu^{2+} exchangeable cations in Cu-ZSM-5, irrespective of their nature, was much greater than that of the Cu^{2+} in Cu-Al-MCM-41, where they are found as CuO.
Keywords: Cu-MCM-41; Cu-ZSM-5; NO reduction; Propane oxidation.

INTRODUCTION

With the objectives to minimise the amount of nitrogen oxides (NO_x) emitted into the atmosphere and to develop a catalyst which could have better performance in the conversion of this type of pollutant into N_2, different metal-exchanged microporous molecular sieves have been studied. In this field, the first work was carried out by Iwamoto (1994), who found that Cu-exchanged ZSM-5 zeolites catalysts were active in the reduction of NO to N_2 with small quantities of light hydrocarbons such as C_2H_4 and C_3H_6 and an excess of O_2. MFI, MOR and FAU zeolites are the most frequently studied aluminium-silicate microporous structures (Kikuchi and Yogo, 1994).

In the nineties, with the synthesis of the MCM-41 mesoporous molecular sieve (Beck et al., 1992), several studies were directed towards application of these types of solids in separation and catalysis processes (Melo et al., 2000; Trong On et al., 2001). The most interesting characteristic of these materials, which have mesopores with diameters between 2.0 and 10.0 nm, is their large specific surface areas, with values on the order of 1,000 m^2/g. In contrast with other mesoporous materials, like activated

*To whom correspondence should be addressed

carbon and aerogels, the ordered mesoporous (metallo)silicates described by Beck et al. (1992) have a narrow pore size distribution. For example, a typical MCM-41 material shows exclusively mesopores of around 4 nm with a pore size distribution with a width at half height of approximately 0.4 nm (Beck et al., 1992).

The appeal of the formation mechanism of these mesoporous silicates is its simplicity, which easily permits modification of pore diameters and the composition of the solid obtained. The templates used in MCM-41 synthesis are surfactants characterised by a long hydrophobic chain and a hydrophilic head group. In an aqueous reaction medium, these surfactants form worm-like micelles, which by self-aggregation generate arrays, e.g. hexagonal arrays in the case of MCM-41. In the presence of adequate inorganic oxide precursors, such as SiO_2, petrification of the liquid crystal structure occurs by precipitation of these oxides between the cylindrical micelles. Removal of surfactant molecules by calcination or solvent extraction produces ordered porous materials, since pore diameters can be tailored by suitable choice of the surfactant (Beck et al., 1992).

In this context and with the aim to verify the use of this type of mesostructured material in the treatment of NO emissions, in this work a |Cu|[SiAl]-MCM-41 mesoporous material was prepared and its properties and catalytic behaviour compared with those of |Cu|[SiAl]-MFI catalysts, which are usually used as reference in the selective catalytic reduction of NO with hydrocarbons.

EXPERIMENTAL

Denominations of the samples prepared in this study were based on IUPAC recommendations (McCusker et al., 2001) as $|M_x|[Si_yAl]$-ZZZ, where M represents the hosted metal specie, x the metal/Al ratio, y the Si/Al ratio and ZZZ the structure type, i.e. MFI for microporous ZSM-5 and MCM-41 for the mesoporous material.

The precursor $|Na_1|[Si_{23}Al]$-MCM-41 mesoporous molecular sieve and $|Na_1|[Si_yAl]$-MFI zeolite were prepared in accordance with the procedures utilized by Melo et al. (2001) and Batista (1997), respectively. $|Cu_x|[Si_yAl]$-MCM-41 and $|Cu_x|[Si_yAl]$-MFI catalysts were prepared by ion exchange at room temperature, utilising a solution of copper acetate (0.033 mol/L). After ion exchange the samples were filtered, washed with deionised water and dried at 110 ^oC during 12 h. A reference sample was also prepared by mixing copper oxide and the precursor $|Na_1|[Si_{11}Al]$-MFI. The solid mixture was subsequently calcined at 500 ^oC for 2 h and the solid obtained was denominated as $|CuO_{0.15}|[Si_{11}Al]$-MFI. The CuO used was prepared by calcination of copper acetate (Aldrich 99 %).

The samples obtained were characterised by X-ray diffraction (XRD), atomic absorption spectroscopy (AAS), nitrogen sorption measurements, UV-diffuse reflectance spectroscopy (DRS-UV), analysis of adsorbed CO by diffuse reflectance IR spectroscopy (DRIFTS) and temperature-programmed reduction by H_2 (H_2-TPR). The XRD analyses were performed on a Siemens D500 diffractometer, using nickel-filtered Cu-?$_\alpha$ radiation and a goniometer velocity of 2° (2Θ)/min. The N_2 sorption measurements of the sample previously treated at 150 ^oC for 2 h under vacuum were made at the temperature of liquid N_2 on Nova-1200 equipment (Quantachrome Corporation). The specific surface area (S_{BET}) of $|Na_1|[Si_{23}Al]$-MCM-41 and $|Cu_{5.7}|[Si_{23}Al]$-MCM-41 was calculated by the BET method (Brunauer et al., 1938) from the amount of adsorbed N_2 in the range of $0.06 < P/P_0 < 0.24$. The mean diameter of the mesopores (d_{mp}) in $|Cu_{5.7}|[Si_{23}Al]$-MCM-41 was determined by the model of BJH (Barret et al., 1951).

DRS-UV analyses were conducted at room temperature on a Varian Cary 5G spectrometer equipped with a diffuse reflection cell. A Teflon sample holder, a quartz window and a Teflon standard were used as reference material. Prior to analysis, the samples were dried at 110 ^oC for 24 h. The resultant reflections (R) were treated with the function of Schuster-Kubelka-Munk, which is represented by the equation $F(R) = 100(1-R)^2/2R$. For the DRIFTS analysis, an infrared spectrometer Nicolet 750 with a spectral resolution of 4 cm^{-1} was used. The samples were pretreated *in situ* at 450 ^oC under O_2 flow (2 % in N_2, v/v) and subsequently cooled to 25 ^oC. Before the adsorption of CO, Cu^{2+} ions were reduced to Cu^+ at 220 ^oC using a H_2 flow (25% in N_2, v/v). The CO (99.997 %) was adsorbed at 25 ^oC, feeding in pulses of CO until the surface was saturated (P_{CO} = 28 Torr) and then removing the excess under N_2 flow. During the DRIFTS experiment, 128 scans were accumulated. The band obtained at 2157 cm^{-1} was deconvoluted with the software Origin 5.0 Peak Fitting using a model of the voigt curve and a constant width at half height.

H_2-TPR analyses were carried out on Micromeritics 2705 equipment having a thermal conductivity detector. An H_2 flow (5% in N_2, v/v, 30

mL/min) and a heating rate of 10 °C/min were used. Prior to analysis the sample (100 mg) was treated at 200 ºC under He flow for 1 h.

$|Cu_{5.7}|[Si_{23}Al]$-MCM-41 and $|Cu_x|[Si_yAl]$-MFI catalysts were evaluated in the reduction of NO to N_2 using propane as reducing agent. Prior to reaction, the catalyst was activated for one hour under air flow at 500 °C and subsequently cooled to room temperature. The feed containing an excess of O_2 (simulating an exhaust gas mixture) had a composition of 0.30 % NO, 0.32 % C_3H_8 and 1.8 % O_2 balanced in He (v/v). The reaction temperature was varied between 200 and 500 °C and a gas space velocity (GHSV) of 42,000 h^{-1}, which was calculated considering the total gas flow, was used. To avoid hot spots, a mass of 50 mg of dry catalyst was homogeneously mixed with 150 mg of α-quartz. The products were analysed using a gas chromatograph (Shimadzu-GC-17A) equipped with a flame ionisation detector (FID) and a thermal conductivity detector (TCD) and three chromatographic columns, one capillary (Al_2O_3/KCl, 30 m × 0.32 mm) and two packed, a Hayesep D (3 m × 1/8") and a Chromossorb 102 (5 m × 1/8").

The activity of the catalysts in propane oxidation was expressed in terms of its total conversion, taking into account the carbon balance during the reaction. In the case of the reduction of NO, its conversion to N_2 was calculated using the following equation: X_{NO} (%) = 2 $[N_2] \times 100/[NO]_o$, where $[N_2]$ is moles of N_2 formed and $[NO]_o$ is moles of NO fed into the reactor.

RESULTS AND DISCUSSION

Characterisation

In Table 1 the Cu content (% Cu w/w) and the Cu/Al ratio of the prepared $|Cu_x|[Si_yAl]$-MFI and $|Cu_{5.7}|[Si_{23}Al]$-MCM-41 catalysts are shown. It can be verified that $|Cu_{0.46}|[Si_{11}Al]$-MFI and $|Cu_{0.28}|[Si_{23}Al]$-MFI samples have lower Cu contents than those corresponding to the maximal ion-exchange capacity (when the ratio of charge-compensating Cu^{2+} per framework Al is 0.5). However for the $|Cu_{5.7}|[Si_{23}Al]$-MCM-41 mesoporous molecular sieve, which was obtained utilising the same ion-exchange procedure, the Cu^{2+}/Al ratio was much higher than 0.5. The different behaviour referred to is probably due to the large hydration sphere of Cu^{2+} cations, which hampers adsorption onto the micropores of ZSM-5 but not onto the mesopores of MCM-41. The Cu^{2+}/Al ratio of 5.7 observed for Cu/MCM-41 suggests the presence of CuO in the solid, while for Cu/ZSM-5, Cu^{2+} cations on ion-exchange sites seem to be more likely.

Table 1: Cu contents and Si/Al and Cu/Al ratios in the prepared $|M_x|$[SiAl]-MFI and $|M_x|$[SiAl]-MCM-41 catalysts (M = Na or Cu).

Sample	Si/Al	Exchange* ´ Exchange time [h]	Cu/Al	Cu [% (w/w)]
$\|Na_1\|$**[**SiAl**]-MFI**	11	--	--	--
$\|Cu_{0.46}\|$**[**Si_{11}Al**]-MFI**	11	3 × 24	0.46	4.8
$\|Cu_{0.28}\|$**[**Si_{23}Al**]-MFI**	23	3 × 6	0.28	0.7
$\|CuO_{0.15}\|$**[**Si_{11}Al**]-MFI**	11	--	0.15	1.6
$\|Na_1\|$**[**Si_{23}Al**]-MCM-41**	23	--	--	--
$\|Cu_{5.7}\|$**[**Si_{23}Al**]-MCM-41**	23	2 × 24	5.7	9.0

*****Number of exchanges.

The XRD patterns for calcined $|Na_1|[Si_{23}Al]$-MCM-41 and activated $|Cu_{5.70}|[Si_{23}Al]$-MCM-41 (Figure 1a) and $|Cu_{0.46}|[Si_{11}Al]$-MFI (Figure 1b) are typical of the molecular sieves studied (Beck et al., 1992; Treacy et al., 1996) and do not indicate the presence of other phases. Although solid-state ion exchange might have occurred in $|CuO_{0.15}|[Si_{11}Al]$-MFI, the presence of reflections of CuO whit their principal diffraction peaks at 35.7 and 38.5° (2Θ) (see Figure 1b), suggests that in this sample Cu^{2+} cations on ion-exchange sites are unlikely. On the other hand, with XRD no crystalline CuO is observed in $|Cu_{0.46}|[Si_{11}Al]$-MFI, suggesting that in this catalyst, most of the Cu cations might be located on ion-exchange sites. Although the high Cu/Al ratio in $|Cu_{5.7}|[Si_{23}Al]$-MCM-41 strongly indicates the presence of non-ionic copper oxide species, in its XRD pattern it is not possible to observe the presence of peaks corresponding to copper oxide. However, this result does not exclude the possibility that this oxide may be present as small CuO crystals with diameters ≤ 3 nm (Carniti et al., 2000), which must be finely dispersed on the mesopore walls.

The decreased intensity of the XRD reflections of

MCM-41 observed after ion exchange (Figure 1a) is due to the adsorption of the radiation by the deposited Cu species rather than to structural degradation. This is also suggested by the nearly unchanged unit cell parameter a_0 of the hexagonally mesoporous arrangement of MCM-41 (Beck et al., 1992) (Table 2) and by the decrease in intensity of the broad peak around 23° (2Θ), typical of amorphous material, which should be increased by structural degradation. The presence of CuO species deposited on the internal pore surface of the MCM-41 structure is also indicated by the increase in wall thickness (ε) and by the decrease in mesopore area (S_p), total pore volume (V_T) and mesopore volume (V_{mp}) of $|CuO_{5.7}|[Si_{23}Al]$-MCM-41, as can be seen from data given in Table2.

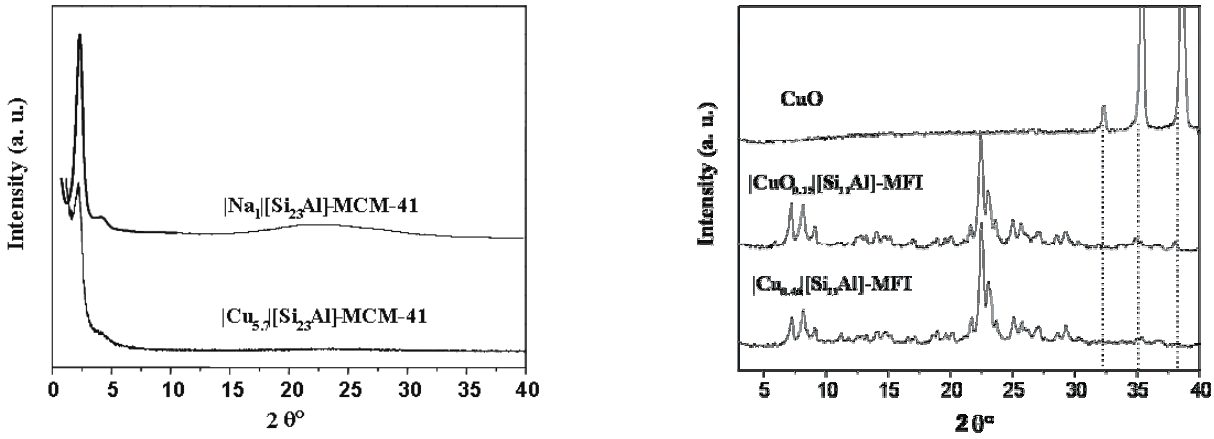

Figure 1: XRD patterns of: (a) $|Na_1|[Si_{23}Al]$-MCM-41 and $|Cu_{5.7}|[Si_{23}Al]$-MCM-41, (b) CuO, $|CuO_{0.15}|[Si_{11}Al]$-MFI and $|Cu_{0.46}|[Si_{11}Al]$-MFI.

Table 2: Structural and textural properties of the prepared MCM-41 mesoporous molecular sieves.

Sample	a_0 [nm]	d_{mp} [nm]	e [nm]	S_{BET} [m^2/g]	S_P [m^2/g]	V_t [cm^3/g]	V_{mp} [cm^3/g]
$\|Na_1\|$**[**$Si_{23}Al$**]-MCM-41**	4.516	2.997	1.519	910	820	9.93	0.74
$\|Cu_{5.7}\|$**[**$Si_{23}Al$**]-MCM-41**	4.533	2.586	1.948	682	453	0.81	0.41

S_p: primary mesopore area; $S_p = S_{total}-S_{ext}$

The results of H_2-TPR (Figure 2) reveal that in $|Cu|[Si_{23}Al]$-MCM-41 as well as in $|CuO_{0.15}|[Si_{11}Al]$-MFI the Cu (II) cations are reduced in one step, as is typical for CuO, thus confirming that this compound is practically the only Cu species present in these samples and that no important solid-state ion exchange occurred after the thermal treatment applied in the samples discussed. The presence of CuO crystals in $|Cu_{5.7}|[Si_{23}Al]$-MCM-41 that are smaller than those in $|CuO_{0.15}|[Si_{11}Al]$-MFI is indicated by the decrease in reduction temperature, which is in accordance with the absence of X-ray reflections attributable to CuO mentioned above.

As can be seen in Figure 2, the H_2-TPR profiles show three reduction peaks for $Cu_{0.46}|[Si_{11}Al]$-MFI and $Cu_{0.28}|[Si_{23}Al]$-MFI catalysts. In accordance with the results reported by Wichterlová et al. (1997), we attributed these peaks to the step-wise reduction of two different kinds of Cu cations (Cu_α and Cu_β) as demonstrated in Table 3, Cu_α has a high positive charge density and therefore is more difficult to be reduced, and is thus found on ZSM-5 zeolites with a low Cu content. On the other hand, Cu_β has a low positive charge density, and therefore is easier to be reduced, and is thus found on ZSM-5 zeolites with a high Cu content. Taking into account the above statements, we attributed the first reduction peak at around 210 ºC to the reduction of Cu_α^{+2} and Cu_β^{+2} to Cu_α^{+1} and Cu_β^{+1}, respectively. The reduction of the latter cations occurred at around 380 ºC for Cu_β^{+1} and at around 580 ºC for Cu_α^{+2}.

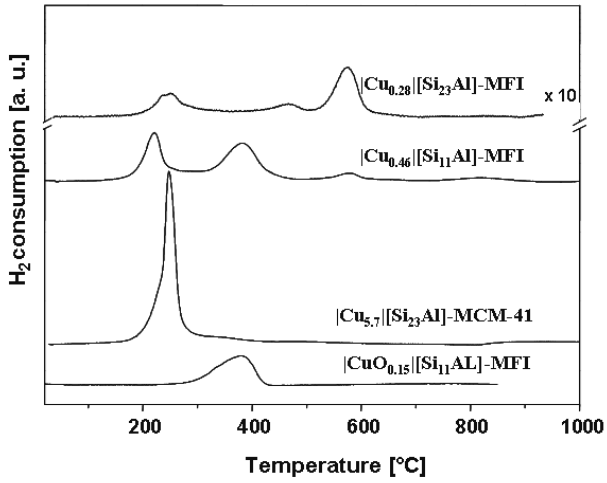

Figure 2: H2-TPR profiles for |Cux|[SiyAl]-MFI, |CuO0.15|[Si11Al]-MFI and |Cu5.70|[Si23Al]-MCM-41 catalysts.

Table 3: Reduction temperatures of Cu cations and the proportion of Cu_a and Cu_b in Cu-exchanged ZSM-5 zeolites.

Sample	Cu_a^{2+} and Cu_b^{2+} to Cu_a^{+} and Cu_b^{+}	Cu_b^{+} to Cu_b^{0}	Cu_a^{+} to Cu_a^{0}	Cu_a^{*} (%)	Cu_b^{*} (%)
$Cu_{0.46}$|[Si_{11}Al]-**MFI**	210 °C	400 °C	600 °C	22	78
$Cu_{0.28}$|[Si_{23}Al]-**MFI**	220 °C	490 °C	600 °C	30	70

*Calculated from H2-TPR profile (Figure 2)

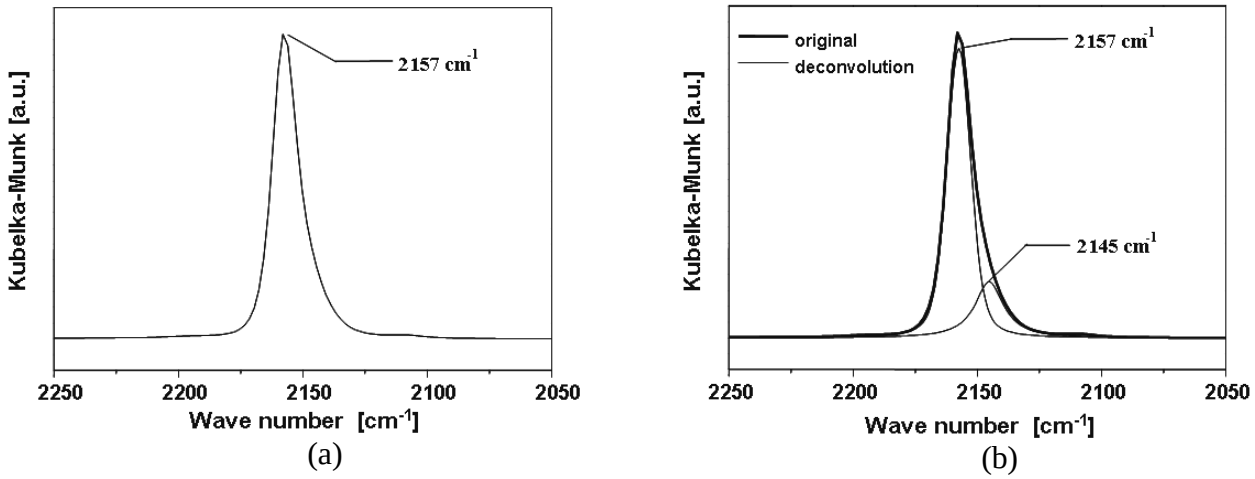

Figure 3: DRIFTS spectra of the adsorption of CO on |$Cu_{0.46}$|[Si_{11}Al]-MFI catalyst: (a) after reduction at 220 °C; (b) deconvolution of the original band.

For all the samples analysed the ratio of consumed H2 to Cu atom (H2/Cu) was nearly one, indicating that all the Cu atoms were effectively reduced. The reduction of Cuα2+ or Cuβ2+ in two steps, observed in sample |Cu0.46|[Si11Al]-MFI, was confirmed by DRIFTS (Figure 3), by which the behaviour of the adsorption of CO on the |Cu0.46|[Si11Al]-MFI catalyst was verified. The resulting spectrum has a band at 2157 cm-1, corresponding to the adsorption of CO on Cu+ cations (Hadjiivanov and Knözinger, 2000).

The deconvolution of the band at 2157 cm-1 is shown in Figure 3b. As can be seen, that band is a consequence of the superposition of two others, a

more intense band at 2157 cm-1 and another at 2145 cm-1. Taking into account the H2-TPR data discussed previously, these bands can be attributed to Cuβ+ and Cuα+, respectively. The Cuβ+-CO species has a higher electron density in the d orbital than the Cuα+-CO species, resulting in an increase in the occupation of the 2 π* orbital and in a weakening of the C=O bond for the former, and thus a shifting of the band to a lower frequency (band at 2145 cm-1 in Figure 3b).

The relative amount of each of these Cu+ cations, obtained from the relative intensity of its respective band in the deconvoluted DRIFTS spectrum, was 23 % for Cuα2+ and 77 % for Cuβ2+, values very similar than those obtained from H2-TPR data (Table 2).

The N_2 adsorption and desorption isotherms for $|Na_1|[Si_{23}Al]$-MCM-41 and $|Cu_{5.70}|[Si_{23}Al]$-MCM-41 samples are shown in Figure 4a, while in Figure 4b the distribution of mesopore diameters as a function of volume of adsorbed N_2 is shown. In Figure 4a it can be observed that both samples have the textural characteristics of mesoporous solids (Janicke et al., 1994). The isotherms observed are of type IV and have a visible step for a relative pressure between 0.2 and 0.4, indicating the condensation of N_2 in the primary mesopores, as is typical for the case of ordered mesopores (Cui et al., 1997). However, this condensation was lower in the $|Cu_{5.70}|[Si_{23}Al]$-MCM-41 sample, thus suggesting the presence of precipitated CuO on the mesopore walls. Therefore, the reduction in specific surface area (S_{BET}) of 25 %, as well as the reduction in mesopore surface (S_P) and primary mesopore volume (V_{mp}) observed for $|Cu_{5.70}|[Si_{23}Al]$-MCM-41 (Table 2), compared to $|Na_1|[Si_{23}Al]$-MCM-41, is also related to its high Cu content (Table 1). This fact is also evident from the diminution in pore diameter, as can be observed in Figure 4b. These results are in accordance with those published by Minchev et al. (2001), who found that the surface area of $|Cu_x|[Si_yAl]$-MCM-41 mesoporous solids is influenced by Cu content and by the method used during Cu impregnation.

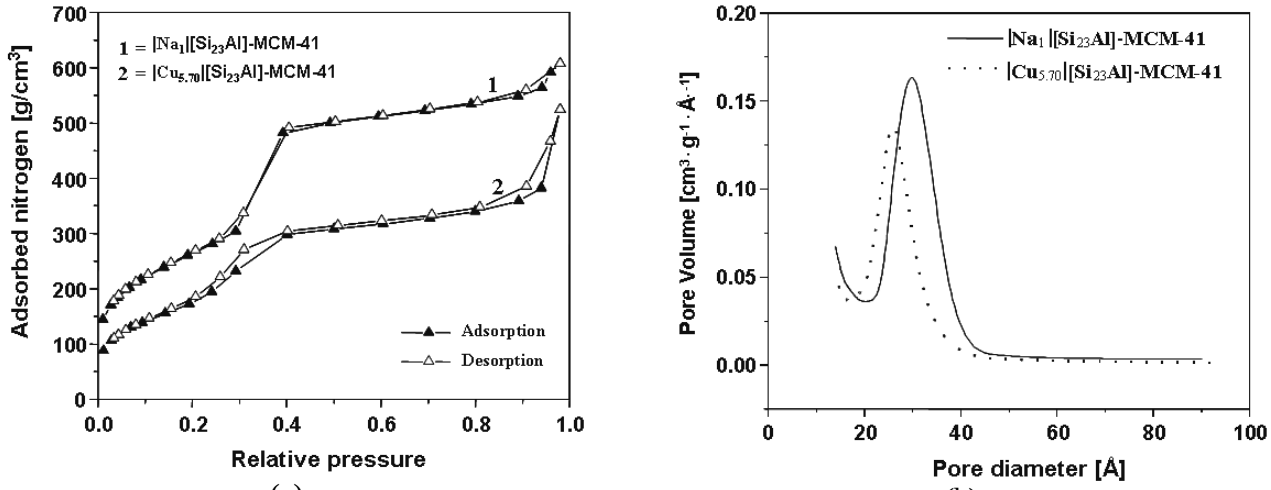

(a) (b)

Figure 4: (a) N_2 adsorption/desorption isotherms; (b) distribution of pore diameters in $|Cu_{5.70}|[Si_{23}Al]$-MCM-41 and $|Na_1|[Si_{23}Al]$-MCM-41 samples.

In Figure 5 the DRS-UV spectra for $|Cu_{5.7}|[Si_{23}Al]$-MCM-41 and $|Cu_x|[Si_yAl]$-MFI samples are shown. It can be observed that irrespective of the type of solid, the Cu-containing samples have bands at 215, 260 and 750 nm. For $|Na_1|[Si_{23}Al]$-MFI, only the first band at 215 nm was observed; therefore it was attributed to structural Al-O units in this material. However, the intensity of this band increases with the increase in Cu content in the sample. In accordance with data published by Teraoka et al. (2000), irrespective of the symmetry of Cu^{2+}cations, the bands at 215 and 260 nm, correspond to the charge transfer transition between the O and the metal ($O \rightarrow Cu^{2+}$). The band at around 750 nm corresponds to d-d electron transitions of Cu^{2+} hexagonally coordinated by water molecules and O atoms found in the framework of the molecular sieves studied (Itho et al., 1994). In accordance with Moretti et al. (2001), this band disappears when $|Cu_x|[Si_yAl]$-MFI-type solids are treated under vacuum at 500 ^oC. As can be seen in Figure 5a, the band at around 890 nm confirms the presence of CuO in $|Cu_{5.7}|[Si_{23}Al]$-MCM-41 (Dossi et al., 1999).

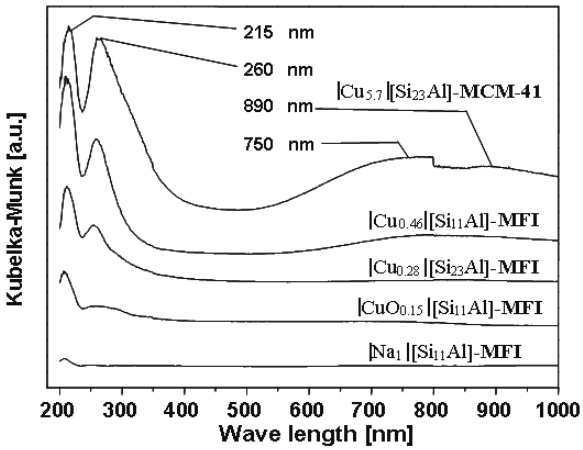

Figure 5: DRS-UV spectra of $|Cu_{5.70}|[Si_{23}Al]$-MCM-41 and $|Cu_x|[Si_yAl]$-MFI samples.

In Figure 6a the results for the selective catalytic reduction of NO to N_2 using propane as reducing agent on $|Cu_x|[Si_yAl]$-MFI, $|Cu_{5.7}|[Si_{23}Al]$-MCM-41 and $|CuO_{0.15}|[Si_{11}Al]$-MFI catalysts are shown. For $|Cu_x|[Si_yAl]$-MFI samples, the conversion of NO was a function of Cu content in the solid (Table 1). Thus, the $|Cu_{0.46}|[Si_{11}Al]$-MFI catalyst with the highest Cu content had a higher conversion than $|Cu_{0.28}|[Si_{23}Al]$-MFI.

The low conversion of NO to N_2 (Figure 6a) and of propane (Figure 6b) on $|CuO_{0.15}|[Si_{11}Al]$-MFI indicates that CuO does not have significant activity for these reactions and that in Cu-based catalysts the Cu cationic species located in extra-framework exchange positions are responsible for the catalytic activity.

This behaviour can be best observed by comparing the activity of $|Cu_{5.7}|[Si_{23}Al]$-MCM-41 and $|Cu_{0.28}|[Si_{23}Al]$-MFI samples (Figure 6), which have very similar values for NO conversion. Although $|Cu_{0.28}|[Si_{23}Al]$-MFI has a much lower copper content than $|Cu_{5.7}|[Si_{23}Al]$-MCM-41 (Table 1), it has Cu atoms, as evidenced by the H_2-TPR results (Figure 2), as cationic species which are compensating the negative charge of the zeolite structure. In contrast, the H_2-TPR results showed that in $|Cu_{5.7}|[Si_{23}Al]$-MCM-41 all the Cu atoms are in the form of CuO (Figure 2). On the other hand, the activity of the latter sample was greater than that of $|CuO_{0.15}|[Si_{11}Al]$-MFI, with this behaviour being attributed to the higher and better dispersed amount of this oxide on the surface of the mesopores.

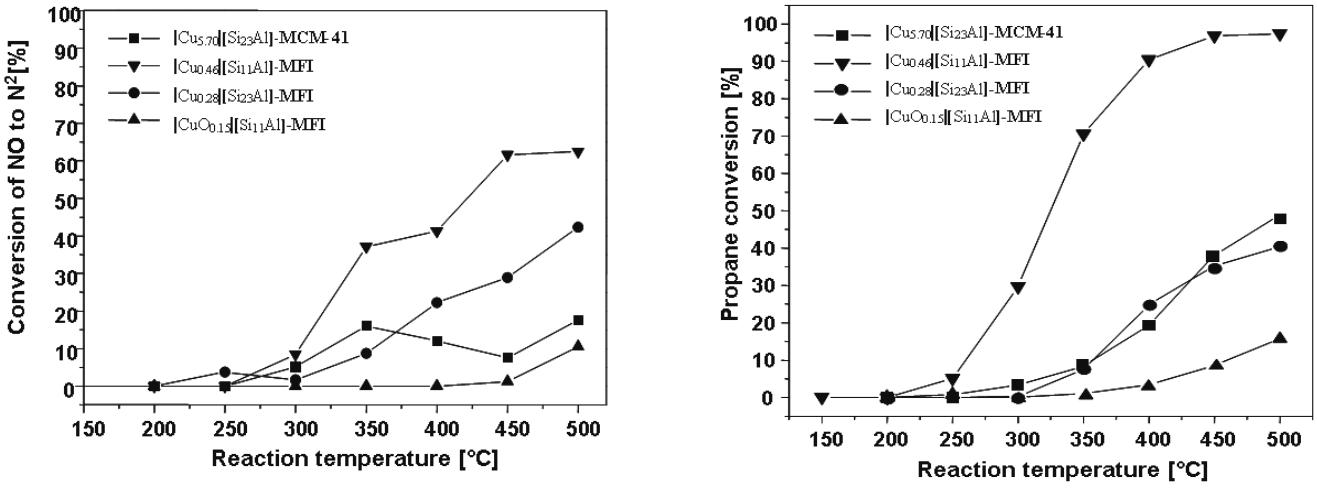

(a) (b)

Figure 6: Conversion of (a) NO to N_2; (b) propane on $|Cu_x|[Si_yAl]$-MFI and $|Cu_{5.70}|[Si_{23}Al]$-MCM-41 catalysts (GHSV = 42,000 h^{-1}).

In Figure 7 the specific activities of the Cu atoms in the catalysts studied are shown for the oxidation of propane ($Cu(spAc)_{propane}$) and for the reduction of NO to N_2 ($Cu(spAc)_{NO}$), calculated as the number of converted molecules per Cu atom per hour. As can be observed, the data for $Cu(spAc)_{NO}$ (Figure 7a) and $Cu(spAc)_{propane}$ (Figure 7b) confirm the discussion of the results plotted in Figure 6, verifying that the Cu atoms in $|Cu_x|[Si_yAl]$-MFI catalysts, irrespective of their nature (Cu_α^{2+} or Cu_β^{2+}), have greater specific activity in both reactions studied than those obtained for Cu atoms in $|Cu_{5.7}|[Si_{23}Al]$-MCM-41 and $|CuO_{0.15}|[Si_{11}Al]$-MFI. Moreover, in the latter catalyst the Cu atoms have practically null specific activity in the reactions discussed.

In Figure 7it can be further observed that for a space velocity (GHSV) of 42,000 h^{-1} and for temperatures higher than 400 °C, the $|Cu_{0.28}|[Si_{23}Al]$-MFI sample has higher values of $Cu(spAc)_{propane}$ and $Cu(spAc)_{NO}$ than $|Cu_{0.46}|[Si_{11}Al]$-MFI. However, under these operating conditions, $|Cu_{0.46}|[Si_{11}Al]$-MFI has propane conversions of 100%, and therefore its specific activity remains constant up to 400 °C (Figure 7b). Increasing the space velocity from 42,000 h^{-1} to 84,000, the $Cu(spAc)_{propane}$ on $|Cu_{0.46}|[Si_{11}Al]$-MFI increased from 25 to 48.5 at 400 °C and to 58.7 at 450 °C (Table 4). These values remained practically constant when the space velocity was changed to 168,000 h^{-1}, indicating that these activity values can be considered as maximal for that catalyst. For the $|Cu_{0.28}|[Si_{23}Al]$-MFI catalyst, which has a lower Cu content, very similar values of $Cu(spAc)_{propane}$ at GHSV=42,000 h^{-1} were obtained (Table 4).

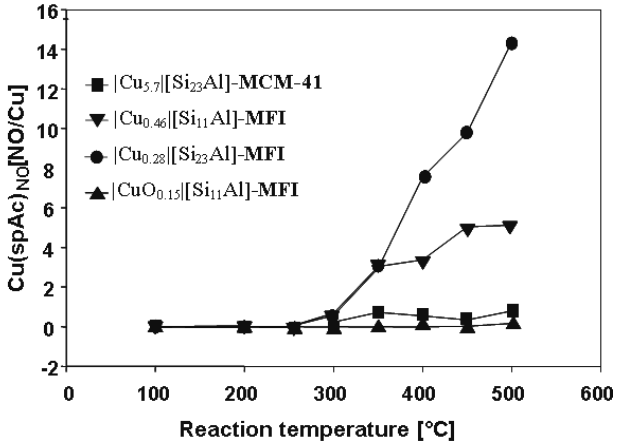

(a)

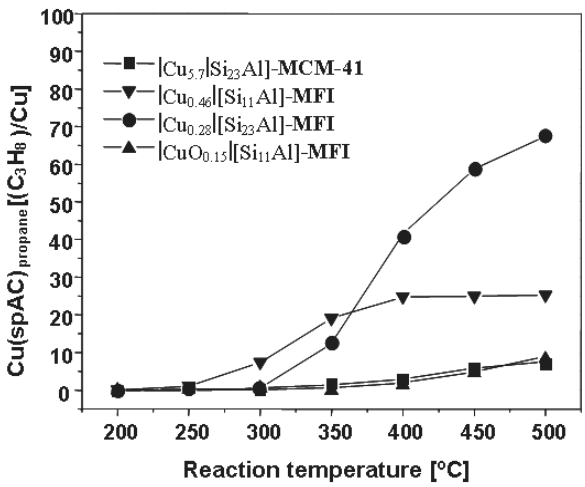

(b)

Figure 7: Specific activity of Cu atoms in (a) the reduction of NO to N_2, $(Cu(spAc)_{NO})$; (b) propane oxidation, $(Cu(spAc)_{propane}$ on $|Cu_x|[Si_yAl]$-MFI and $|Cu_{5.70}|[Si_{23}Al]$-MCM-41 catalysts (GHSV = 42,000 h^{-1}).

Table 4: Specific catalytic activity for propane oxidation ($Cu(spAC)_{propane}$) as a function of GHSV during the reduction of NO on $|Cu_x|[Si_yAl]$-MFI catalysts.

Sample	GHSV [h^{-1}]	42,000		84,000		168,000	
	Temperature [°C]	400	450	400	450	400	450
$\|Cu_{0.46}\|[Si_{11}Al]$-MFI		25	25	48.5	58.7	47.2	55.6
$\|Cu_{0.28}\|[Si_{23}Al]$-MFI		41.4	58.3	-	-	-	-

CONCLUSIONS

H_2-TPR and DRS-UV data demonstrated that in $|Cu_{5.7}|[Si_{23}Al]$-MCM-41 the Cu atoms are in the form of CuO dispersed on the surface of the mesopores, which results in a decrease in peak intensity in the XRD pattern and in a reduction in specific surface area and mesopore volume. On the other hand, data from H_2-TPR and DRIFTS on the adsorption of CO on Cu^+ provided evidence that, depending on Si/Al ratio and Cu content in the zeolite, the copper atoms in Cu-exchanged ZSM-5 zeolites ($|Cu_x|[Si_yAl]$-MFI), coexist as two different Cu^{2+} cations (Cu_α^{2+} or Cu_β^{2+}), which are located in extraframework exchangeable positions and have different thermo-redox properties than Cu atoms in $|Cu_{5.7}|[Si_{23}Al]$-MCM-41.

It was verified that Cu atoms in $|Cu_x|[Si_yAl]$-MFI catalysts have greater specific activities in the conversion of NO to N_2 and in propane oxidation than copper atoms in $|Cu_{5.7}|[Si_{23}Al]$-MCM-41 and $|CuO_{0.15}|[Si_{11}Al]$-MFI. This behaviour confirms that Cu species, which are compensating the negative charge of the zeolite structure, irrespective of their nature (Cu_α^{2+}, Cu_β^{2+}), are responsible for the activity in both reactions.

ACKNOWLEDGEMENTS

The authors gratefully acknowledge the financial support received from Conselho Nacional de Desenvolvimento Científico e Tecnológico for this study (CNPq/Brazil, grants 477759/2003-3 and 551008/2002-4). Dr. M. S. Batista thanks Fundação de Amparo à Pesquisa do Estado de São Paulo, Brazil for his doctoral scholarship (FAPESP, grant 1998/02495-5). The support of Fundação de Amparo à Pesquisa do Estado de Minas Gerais (FAPEMIG/Brazil, grant TEC–1241/01) is also acknowledged.

REFERENCES

Barret, E.P., Joyner, L.G. and Halenda, P.P., The Determination of Pore Volume and Area Distributions in Porous Substances I. Computations from Nitrogen Isotherms, J. Am. Chem. Soc., 73, 373 (1951).

Batista, M.S., Desproporcionamento de Alquil-Aromáticos sobre Zeólitas. M.Sc. thesis, Universidade Federal de São Carlos (UFSCar), São Carlos, Brazil (1997).

Beck, J.S., Vartuli, J.C., Leonowicz, M.E., Kresge, C.T., Schmitt, K.D., Chu, C.T.W., Olson, D.H., Sheppard, E.W., McCullen, S.B., Higgins, J.B. and Schlenker, J.L., A New Family of Mesoporous Molecular Sieves Prepared with Liquid Crystal Templates**,** J. Am. Chem. Soc., 114, 10834 (1992).

Brunauer, S., Emmett, P.H. and Teller, E.J., Adsorption of Gases in Multimolecular Layers, J. Am. Chem. Soc., 60, 309 (1938).

Carniti, P., Gervasini, A., Modica, V H. and Ravasio, N., Catalytic Selective Reduction of NO with Ethylene over a Series of Copper Catalysts on Amorphous Silicas**,** Appl. Catal. B, 28, 175 (2000).

Cui, J., Yue, Y.-H., Sun, Y., Dong, W.-Y. and Gao, Z., Characterization and Reactivity of Ni, Mo-Supported MCM-41-Type Catalysts for Hydrodesulfurization, Stud. Surf. Sci. Catal., 105, 687 (1997).

Dossi, C., Fusi, A., Recchia, S., Psaro, R. and Moretti, G., Cu-ZSM-5 (Si/Al=66), Cu-Fe-S-1 (Si/Fe=66) and Cu-S-1 Catalysts for NO Decomposition: Preparation, Analytical Characterization and Catalytic Activity, Micro- and Mesoporous Mater., 30, 165 (1999).

Gesser, H.D. and Goswami, P.C., Aerogels and Related Porous Materials, Chem. Rev., 89, 765 (1989).

Hadjiivanov, K. and Knözinger, H., FTIR Study of Low-Temperature CO Adsorption on Cu-ZSM-5: Evidence of the Formation of $Cu^{2+}(CO)_2$ Species, J. Catal., 191, 480 (2000).

Itho, Y., Nishiyama, S., Tsuruya, S. and Masai, M., Redox Behavior and Mobility of Copper Ions in NaZSM-5 Zeolite During Oxidation, J. Phys. Chem., 98, 960 (1994).

Iwamoto, M., Zeolites in Environmental Catalysis, Stud. Surf. Sci. Catal., 84, 1395 (1994).

Janicke, M., Kumar, D., Stucky, G. and Chmelka, B.F., Aluminum Incorporation in Mesoporous Molecular Sieves, Stud. Surf. Sci. Catal., 84, 243 (1994).

Kikuchi, E. and Yogo, K., Selective Catalytic Reduction of Nitrogen Monoxide by Methane on Zeolite Catalysts in an Oxygen-Rich Atmosphere, Catal. Today, 22, 73 (1994).

McCusker, L.B., Liebau, F. and Engelhardt, G., Nomenclature of Structural and Compositional Characteristics of Ordered Microporous and Mesoporous Materials with Inorganic Hosts, Pure

Appl. Chem., 73, 381 (2001).

Melo, R.A.A., Batista, M.S. and Urquieta-González, E.A., Atividade Catalítica de Peneiras Moleculares H-Al-SiMCM-41 na Isomerização do *meta*-Xileno. Anais XIII Congresso Brasileiro de Engenharia Química e XIX Interamerican Congress of Chemical Engineering (CD), 2000.

Melo, R.A.A., Batista, M.S. and Urquieta-González, E.A., Estudo das Propriedades Catalíticas da Peneira Molecular Mesoporosa H-Al-MCM-41 através de Reações Modelo. Anais XI Congresso Brasileiro de Catálise e I Congresso de Catálise do Mercosul, Volume 2, 1017 (2001).

Minchev, C., Köhn, R., Tsonsheva, T., Dimitrov, M. and Fröba, M., Preparation and Characterization of Copper Oxide Modified MCM-41 Molecular Sieves, Stud. Surf. Sci. Catal., 135 (CD) (2001).

Moretti, G., Ferraris, G. and Galli, P., Autoreduction of Cu^{2+} Species in Cu-ZSM-5 Catalysts – Studies by Diffuse Reflectance Spectroscopy, X-Ray Photoelectron Spectroscopy, Thermogravimetry and Elemental Analysis, Stud. Surf. Sci. Catal., 135 (CD) (2001).

Ryu, Z.Y., Zheng, J.T., Wang, M.Z. and Zhang, B.J., Characterization of Pore Size Distributions on Carbonaceous Adsorbents by DFT, Carbon, 37, 1257 (1999).

Sing, K.S.W., Reporting Physisorption Data for Gas/Solid Systems With Special Reference to the Determination of Surface Area and Porosity, Pure Appl. Chem., 54, 2201 (1982).

Teraoka, Y., Tai, C., Ogawa, H., Furukawa, H. and Kagawa, S., Characterization and NO Decomposition Activity of Cu-MFI Zeolite Relation to Redox Behavior, Appl. Catal. A: General, 200, 167 (2000)

Treacy, M.M.J., Higgins, J.B. and v. Ballmoos, R., Collection of Simulated XRD Powder Patterns for Zeolites, Zeolites, 16, 323 (1996).

Trong On, D., Desplantier-Giscard, D., Danumah, C. and Kaliaguine, S., Perspectives in Catalytic Applications of Mesostructured Materials, Appl. Catal. A: General, 222, 299, (2001).

Wichterlová, B., Sobalík, Z. and Dedecek, J., Cu Ion Siting in High Silica Zeolites –Spectroscopy and Redox Properties, Catal. Today, 38, 199 (1997).